Atg1-mediated autophagy suppresses tissue degeneration in *pink1/parkin* mutants by promoting mitochondrial fission in *Drosophila*

Peng Ma[a], Jina Yun[b], Hansong Deng[a,b,†,*], and Ming Guo[b,†,*]
[a]Shanghai East Hospital, School of Life Sciences and Technology, Tongji University, Shanghai 20092, China;
[b]Department of Neurology, Department of Molecular and Medical Pharmacology, UCLA David Geffen School of Medicine, and California NanoSystems Institute at UCLA, University of California, Los Angeles, Los Angeles, CA 90095

ABSTRACT **Mitochondrial dysfunction is considered a hallmark of multiple neurodegenerative diseases, including Parkinson's disease (PD). The PD familial genes *pink1* and *parkin* function in a conserved pathway that regulates mitochondrial function, including dynamics (fusion and fission). Mammalian cell culture studies suggested that the *pink1/parkin* pathway promotes mitophagy (mitochondrial autophagy). Mitophagy through mitochondrial fission and autolysosomal recycling was considered a quality control system at the organelle level. Whether defects in this quality control machinery lead to pathogenesis in vivo in PD remains elusive. Here, we found that elevating autophagy by *atg1* overexpression can significantly rescue mitochondrial defects and apoptotic cell death in *pink1* and *parkin* mutants in *Drosophila*. Surprisingly, the rescue effect relied both on the autophagy–lysosome machinery and on *drp1*, a mitochondrial fission molecule. We further showed that Atg1 promotes mitochondrial fission by posttranscriptional increase in the Drp1 protein level. In contrast, increasing fission (by *drp1* overexpression) or inhibiting fusion (by knocking down *mitofusin [mfn]*) rescues *pink1* mutants when lysosomal or proteasomal machinery is impaired. Taken together, our results identified Atg1 as a dual-function node that controls mitochondrial quality by promoting mitochondria fission and autophagy, which makes it a potential therapeutic target for treatment of mitochondrial dysfunction–related diseases, including PD.**

Monitoring Editor
Erika Holzbaur
University of Pennsylvania

Received: Apr 23, 2018
Revised: Oct 17, 2018
Accepted: Oct 19, 2018

INTRODUCTION

Accumulating evidence indicates that mitochondrial dysfunction might have a causative role in Parkinson's disease (PD) pathogenesis (Schapira, 2008). For instance, PD patients have reduced complex I activity, and mitochondrial toxins, such as MPTP and rotenone, can induce acute parkinsonism (Schapira, 1993). Moreover, mutations in the PD-related genes PINK1 and PARKIN cause mitochondrial dysfunction. We and others have previously reported that *Drosophila pink1* and *parkin* genes function in the same genetic pathway, with *pink1* acting upstream of *parkin*, to regulate mitochondrial morphology and tissue maintenance of indirect flight muscles (hereafter referred to as "muscles") and dopaminergic (DA) neurons (Clark *et al.*, 2006; Park *et al.*, 2006; Yang *et al.*, 2006, 2008; Deng *et al.*, 2008; Poole *et al.*, 2008). Studies employing mammalian cell culture and other animal models revealed that the regulation of mitochondrial integrity and function by the *pink1/parkin* pathway is well conserved (Palacino *et al.*, 2004; Exner *et al.*, 2007; Gautier *et al.*, 2008; Flinn *et al.*, 2009; Lutz *et al.*, 2009; Yu *et al.*, 2011).

Mitochondria are dynamic organelles that continually undergo fusion and fission. Dynamin-related protein 1 (Drp1) is a cytosolic GTPase that can assemble around the mitochondrial outer membrane and trigger mitochondrial fission. The GTPases Mitofusion

This article was published online ahead of print in MBoC in Press (http://www.molbiolcell.org/cgi/doi/10.1091/mbc.E18-04-0243) on October 24, 2018.

†These authors contributed equally to this work.

The authors declare no competing financial interests.

Author contributions: P.M., H.D., and M.G. designed the experiments and wrote the manuscript; H.D. and. J.Y. performed experiments and analyzed the data.

*Address correspondence to: Hansong Deng (hdeng@tongji.edu.cn) and Ming Guo (mingfly@ucla.edu).

Abbreviations used: ATG, autophagy-related protein; DA, dopaminergic; MVB, multivesicle body; PD, Parkinson's disease; RNAi, RNA interference.

(Mfn1 and Mfn2) and the optical atrophy 1 (Opa1) mediate fusion of the outer and inner membranes, respectively (Chen and Chan, 2009; Westermann, 2010). Mitochondrial dynamics has been linked to multiple mitochondrial functions, including respiratory capacity, apoptosis, nutritional status, and mitochondrial quality control (Tatsuta and Langer, 2008; Youle and van der Bliek, 2012; Ashrafi and Schwarz, 2013). It was implied that fusion of mitochondria favors their functional repair, while fission leads to elimination of the irreversible damaged organelles (Tatsuta and Langer, 2008; Youle and van der Bliek, 2012). In line with this model, Twig *et al*. (2008) showed in cell culture that mitochondrial fission generated two heterogeneous mitochondria in terms of mitochondrial membrane potential. Hyperpolarized mitochondria can readily fuse with other mitochondria and reenter the network, while severely depolarized ones lose fusion ability and are subsequently degraded by autophagy.

Autophagy mediates the lysosome-dependent turnover of macromolecules and organelles. Macroautophagy is the most extensively studied form of autophagy, involving formation of double membrane vesicles, known as autophagosomes. The (macro) autophagy process consists of the following three major steps: autophagosome formation, maturation through fusion with multivesicle bodies (MVBs)/lysosomes, and degradation of the content within the lysosomes (He and Klionsky, 2009; Chen and Klionsky, 2011). Autophagosome formation is controlled by a series of autophagy-related proteins (ATGs). In all eukaryotes, autophagy is induced via the autophagy-related gene 1 (Atg1) complex (Mizushima, 2010). Expansion of the autophagosome membrane requires two distinct sets of ubiquitin-like protein conjugation systems, Atg8 and Atg5-Atg12. Both systems share one E1-like protein, Atg7 (He and Klionsky, 2009; Mizushima, 2010). A second step is autophagosome maturation. Fusion of autophagosomes and endosomes with lysosomes have converging steps and share common components. For instance, Rab7, a small GTPase, is essential for maturation of autophagosomes/endosomes (Jager *et al*., 2004; Hyttinen *et al*., 2013). Components of the Class C vacuolar protein sorting (Vps-C) complex, such as Carnation (Car) and Vps16, are required for both endosomal trafficking and autophagosome maturation in *Drosophila* (Sevrioukov *et al*., 1999; Sriram *et al*., 2003). The final step is degradation of contents in the autolysosome by lysosomes. The acidic environment inside the lysosome is crucial for the degradation process. The low pH (~4–5) is maintained by ATP-dependent proton pumps, such as vacuole-ATPases (V-ATPases). Inhibition of V-ATPase function causes the failure of acidification of several intracellular compartments, including endosomes and lysosomes. V-ATPases are highly conserved large multisubunit complexes composed of a peripheral domain (V1) responsible for ATP hydrolysis and an integral domain (V0) that carries out the proton transport (Nelson, 2003). *VhaAC39* encodes one of the two V-ATPase V0 d subunits in *Drosophila*. Loss of the *VhaAC39* gene causes loss of acidic compartments and deregulation of endocytosis (Yan *et al*., 2009).

Although generally considered a nonselective process, autophagy can selectively degrade organelles. Recent evidence overwhelmingly indicates that, in mammalian cell lines, Pink1 and Parkin participate in selective degradation of damaged mitochondria by autophagy (Matsuda *et al*., 2010; Narendra *et al*., 2010). In brief, Parkin, an E3 ubiquitin ligase, is recruited by Pink1, a mitochondrial targeted serine–threonine kinase, which was stabilized on chemically uncoupled mitochondria. Ubiquitination of substrates on the outer membranes of mitochondria, including Mfn1, Mfn2 and Miro, facilitates the segregation of severely damaged mitochondrial and halts mitochondrial motility (Chen and Dorn, 2013; Wang *et al*., 2011). Finally, these depolarized mitochondria are removed by proteasome system (UPS) and autophagy machinery, which are recruited by parkin (Chan *et al*., 2011). The canonical ATG pathway is involved in the removal process, as LC3, P62, and ATG5 are required (Kawajiri *et al*., 2010). Clearly, the *pink1/parkin* mediated mitophagy process has been established in cell lines, and it is proposed to play an important role in mitochondrial quality control at the organelle level. However, the physiological significance of mitophagy in terms of regulating *pink1/parkin* associated pathogenesis is still elusive (Whitworth and Pallanck, 2017).

Here, we found mitochondrial autophagy to be beneficial; however, it is dispensable for cell survival and tissue maintenance in *pink1/parkin* mutants in *Drosophila* when mitochondrial fission is simultaneously enhanced.

RESULTS

Overexpression of Atg1 can rescue *pink1/parkin* null mitochondrial defects and muscle degeneration

Pink1^{705} mutants, a null allele of *pink1* (Clark *et al*., 2006; Deng *et al*., 2008) (*pink1^{5}* in short and hereafter), show severe mitochondrial defects in muscles. Wild-type mitochondria are of regular shape and align between the muscle fibers, as indicated by mitochondrial targeted mito::GFP (Figure 1A). *Pink1^{5}* muscles are filled with aberrant clumps of intense mito::GFP signals (Figure 1A). Under transmission electron microcopy (TEM), the mitochondrial cristae in wild-type muscles are densely packed, while *pink1^{5}* mitochondria are swollen with broken cristae (Figure 1B). Mitochondrial defects in *pink1^{5}* were also observed by toluidine blue staining: mitochondria in wild-type muscles were densely stained and dark, while mitochondria of *pink1^{5}* mutants were swollen and faint (Figure 1C). Owing to severe mitochondrial dysfunction, the muscles in *pink1^{5}* mutants degenerate, as indicated by age-dependent accumulation of TUNEL (terminal deoxynucleotidyl transferase dUTP nick end labeling)-positive nuclei and irregular indentation of the external thorax (Figure 1, D and E).

Autophagy is the major route for mitochondrial clearance. In *Drosophila*, overexpression of Atg1 alone is sufficient to increase autophagy (Scott *et al*., 2007; Chang and Neufeld, 2009). We sought to test whether enhancing autophagy by overexpression of Atg1 can rescue *pink1/parkin* muscle degeneration.

Overexpressing Atg1 by panmuscle drivers, Mef2-Gal4 or Mhc-Gal4 using the binary UAS-GAL4 system (Brand and Perrimon, 1993), was lethal (unpublished data). We therefore induced Atg1 overexpression (Atg1^{OE}) using IFM-Gal4, which is an indirect flight muscle–specific driver (Yun *et al*., 2014). Atg1^{OE} muscles had significantly smaller mitochondria than the wild type, and no obvious muscle degeneration was observed in young adults (2–4 d old; Figure 1, A and F). Interestingly, mitochondrial defects in *pink1^{5}* mutants, such as mito::GFP clumps and swollen and broken cristae, were rescued by Atg1^{OE} (Figure 1, A, B, and F). This rescuing effect was confirmed by antibody staining against mitochondrial complex V subunit (Supplemental Figure S1, A–D). Muscle degeneration in *pink1^{5}* mutants, as indicated by TUNEL-positive nuclei and thoracic indentation, was suppressed by Atg1^{OE} (Figure 1, D, E, and G). Furthermore, Atg1^{OE} also rescued mitochondrial defects and muscle degeneration in *parkin^{RNAi}* flies (Figure 1. H, I, L, and M). Overexpressing a kinase-inactive form of Atg1 (UAS::Atg1^{K38Q}) failed to rescue *pink1^{5}* defects (Figure 1, J–M), suggesting that the rescuing effect of Atg1 depends on its kinase activity.

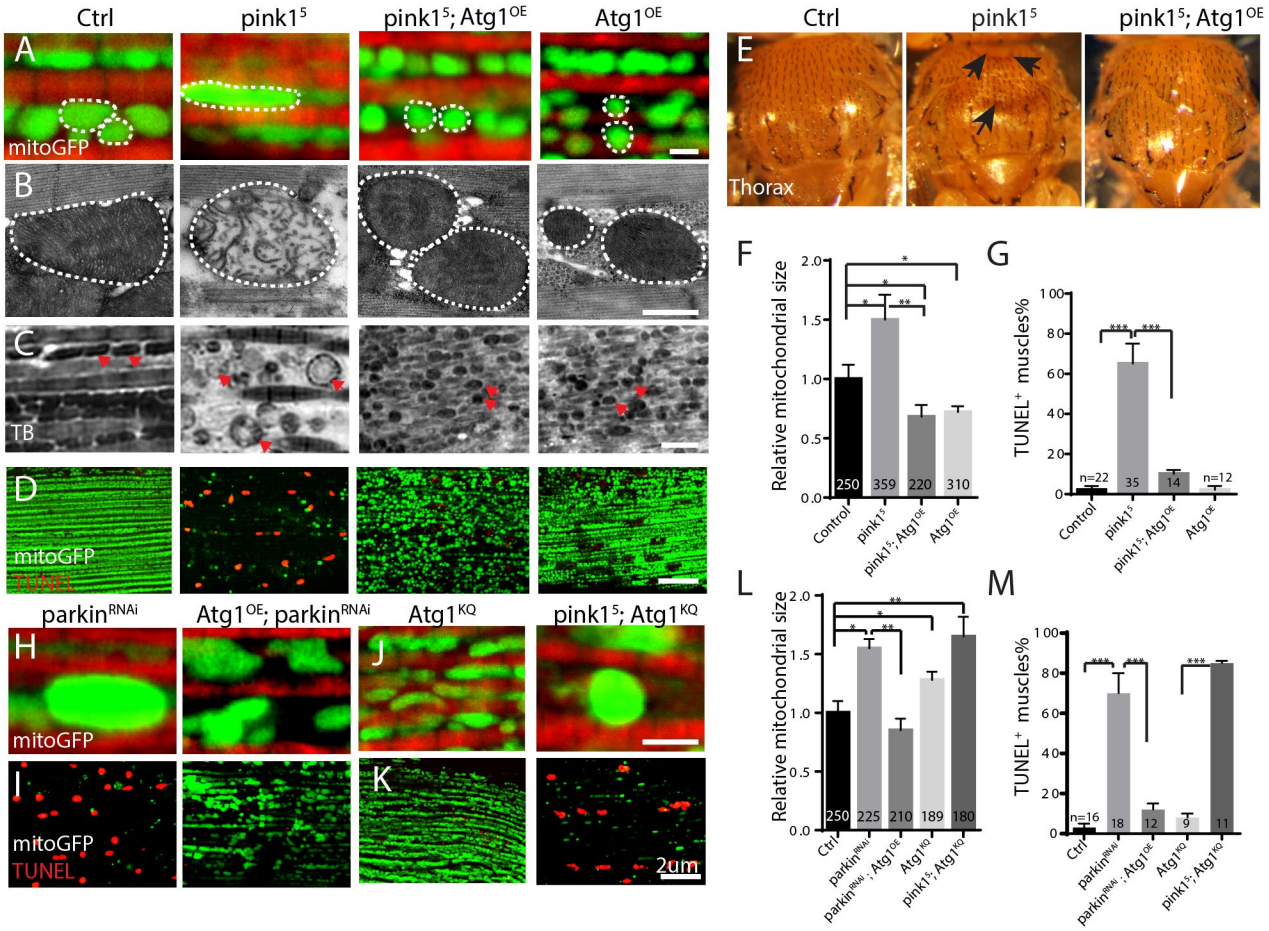

FIGURE 1: Overexpression of Atg1 rescues muscle degeneration in *pink1/parkin* mutants. (A) Mitochondria (mitoGFP in green) in indirect flight muscles (phalloidin stains fiber in red) are visualized under a confocal microscope. (B) TEM analysis of mitochondria in indirect flight muscles of indicated genotypes. (C) Toluidine blue staining of muscle thick section. (D) TUNEL assay (nuclear stains in red). (E) Images of thoraces. Arrows point to thoracic indentations due to muscle degeneration. All *pink1*^{5}-associated defects, including thorax indentation, mitochondrial abnormality, and TUNEL-positive nuclei in muscles, can be rescued by overexpressing Atg1 (IFM-Gal4>UAS::Atg1^{OE}); see A–E. (F) Mitochondria in muscles of indicated genotypes were measured with ImageJ and normalized with controls. Mitochondria from at least 10 animals were analyzed (*N* denoted in the graph). Student's *t* test and SEM are shown. ***$p < 0.001$, **$p < 0.05$, *$p < 0.01$. (G) Quantification of TUNEL-positive muscles in indicated genotypes. Muscles are multinuclear, and all nuclei in a muscle are either TUNEL-positive or -negative. At least 10 flies for each genotype were quantified for statistical analysis. Student's *t* test and SEM are shown. ***$p < 0.001$, **$p < 0.05$, *$p < 0.01$. (H) Mitochondria of indirect flight muscle (IFM) in different genotypes are visualized under confocal microscopy. (I) TUNEL-positive nuclei (red) in *parkin* mutant muscles were rescued by overexpressing Atg1. Mito::GFP (green) labels mitochondria. (J, K) Overexpressing kinase-inactive version of Atg1 (UAS::Atg1^{KQ}) failed to rescue mitochondrial morphology (H) or TUNEL-positive cells (I) of *pink1*^{5} mutant muscles. (L, M) Quantification of mitochondrial size and TUNEL-positive size shown in J and K. Student's *t* test and SEM are presented. ***$p < 0.001$, **$p < 0.05$, *$p < 0.01$.

Functional autophagy machinery is required for phenotypic rescue mediated by Atg1 overexpression

The mitochondrial morphology in *pink1*^{5} muscles correlated closely with cell viability: in viable cells (TUNEL-negative), mitochondrial were elongated and formed big clumps, while in degenerating muscles (TUNEL-positive), the mitochondria were substantially fragmented (Supplemental Figure S2, A–C). We sought to examine autophagy activity in wild-type and *pink1*^{5} muscles. LysoTracker stains acidic cellular compartments, including lysosomes. No obvious LysoTracker-positive vesicle colocalized with mito::GFP in wild-type muscles (Figure 2A), while *pink1*^{5} muscles showed significant increases of LysoTracker staining in both number and size (Figure 2, B and C). Interestingly, in those degenerating *pink1*^{5} muscles, around 30% of the LysoTracker-positive vesicles colocalized with mito::GFP (Figure 2, B and D). In both cases, a subset of mito::GFP was adjacent to LysoTracker-positive vesicles (Figure 2, B and C). Colocalization of mitoGFP with LysoTracker implied either blockage or enhanced mitochondrial autophagy (Klionsky *et al.*, 2008); however, LysoTracker was found inside the mitochondria, often with faint mito::GFP (arrows in Figure 2B), indicating that mitochondria are degrading inside lysosomes.

To further distinguish between these two possibilities, we introduced an autophagy reporter, mCherry-GFP-Atg8, in which GFP but not mCherry is quenched inside acid lysosomes (Mauvezin *et al.*, 2015). Significantly more GFP^{+} Cherry^{+} and GFP^{-} Cherry^{+} positive vesicles were observed in *pink1*^{5} mutants, indicating augmented autophagy (Figure 2F and Supplemental Figure S5). Overexpression of Atg1 (Atg1^{OE}) induced autophagy in *pink1*^{5} mutants, as indicated

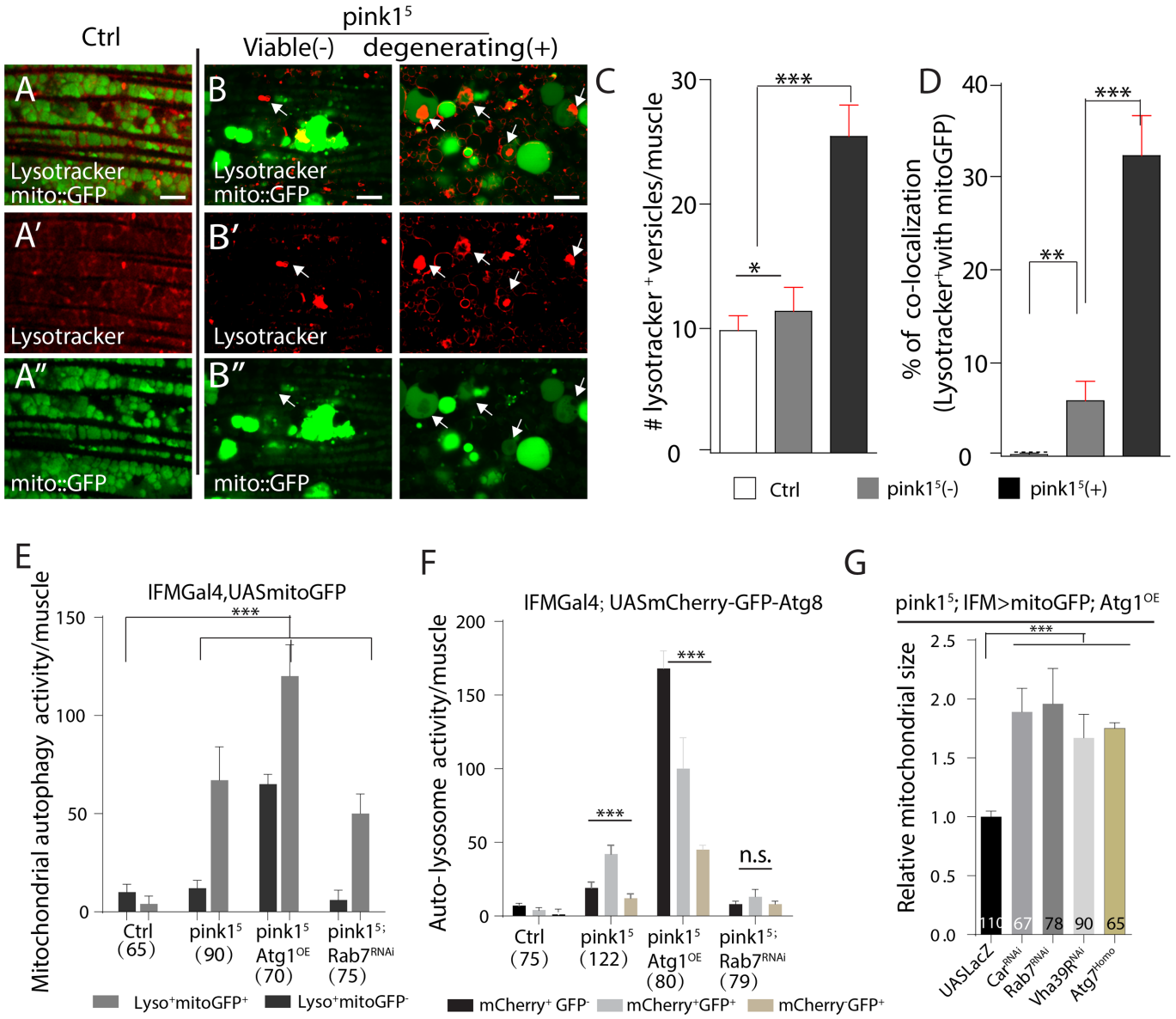

FIGURE 2: Functional autophagy machinery is required for Atg1 overexpression-mediated rescuing effect on *pink1* mutants. (A, B) Acidic compartments (stained by LysoTracker in red) and mitochondria (mito::GFP in green) in freshly dissected muscles. Arrows point to potential colocalization of mito::GFP and LysoTracker. "Viable (–)" muscles in *pink1* mutants have large mitoGFP clumps and are always TUNEL-negative. In "degenerating (+)" muscles, mito::GFP clumps are replaced by "fragmented" mitochondria and are always TUNEL- positive (see also Supplemental Figure S2 and main text for details). (C) Quantification of LysoTracker-positive vesicles with diameter greater than 0.2 μm in muscles. (D) Percentage of LysoTracker-positive vesicles showing colocalization with mito::GFP in *pink1*^{5} muscles. In both C and D, *pink1*^{5}(–) means viable muscle, while *pink1*^{5} (+) means degenerating muscles. At least 20 muscles from 5–6 male flies were counted. ***$p < 0.001$, *$p < 0.05$ (unpaired *t* test). (E) Mitochondrial autophagy activity was quantified based on localization of LysoTracker and mitoGFP. Number of events counted for each genotype is labeled under the chart. (F) Autophagic activity was measured based on the genetic reporter UASmCherry-GFP-Atg8. mCherry$^+$GFP$^-$, mCherry$^+$GFP$^+$, and mCherry$^-$GFP$^+$ were measured separately. Events counted for each condition are indicated. (G) Autophagy is required for Atg1^{OE} rescuing effect on *pink1* mutants. Mitochondrial size was normalized with controls. At least 100 mitochondria from more than 10 animals were counted and analyzed for each genotype. For E, F, G, one-way analysis of variance (ANOVA) was performed for statistical analysis. SEM and *p* value are shown: ***$p < 0.001$, **$p < 0.01$, *$p < 0.05$.

by the increase in LysoTracker-positive vesicles (Figure 2, E and F, and Supplemental Figures S3 and S4).

To test whether autophagy is required for the rescuing effect of Atg1^{OE} on *pink1*^{5} mutants, components of the autophagy pathway were inhibited in the *pink1*^{5}; Atg1^{OE} background. Atg7 is essential for autophagy induction, and flies lacking Atg7 are viable, although autophagy was severely impaired (Juhasz *et al.*, 2007). As expected, null mutants of *atg7*$^{d14/d77}$ blocked the Atg1^{OE}-rescuing effect in *pink1*^{5} muscles (Figure 2G and Supplemental Figure S5). Rab7 (YFP-fused Rab7 under UAS control) expressed in muscles readily colocalizes with LysoTracker, indicating that Rab7 is involved in endolysosomal trafficking (Supplemental Figure S6A). Indeed, knockdown of

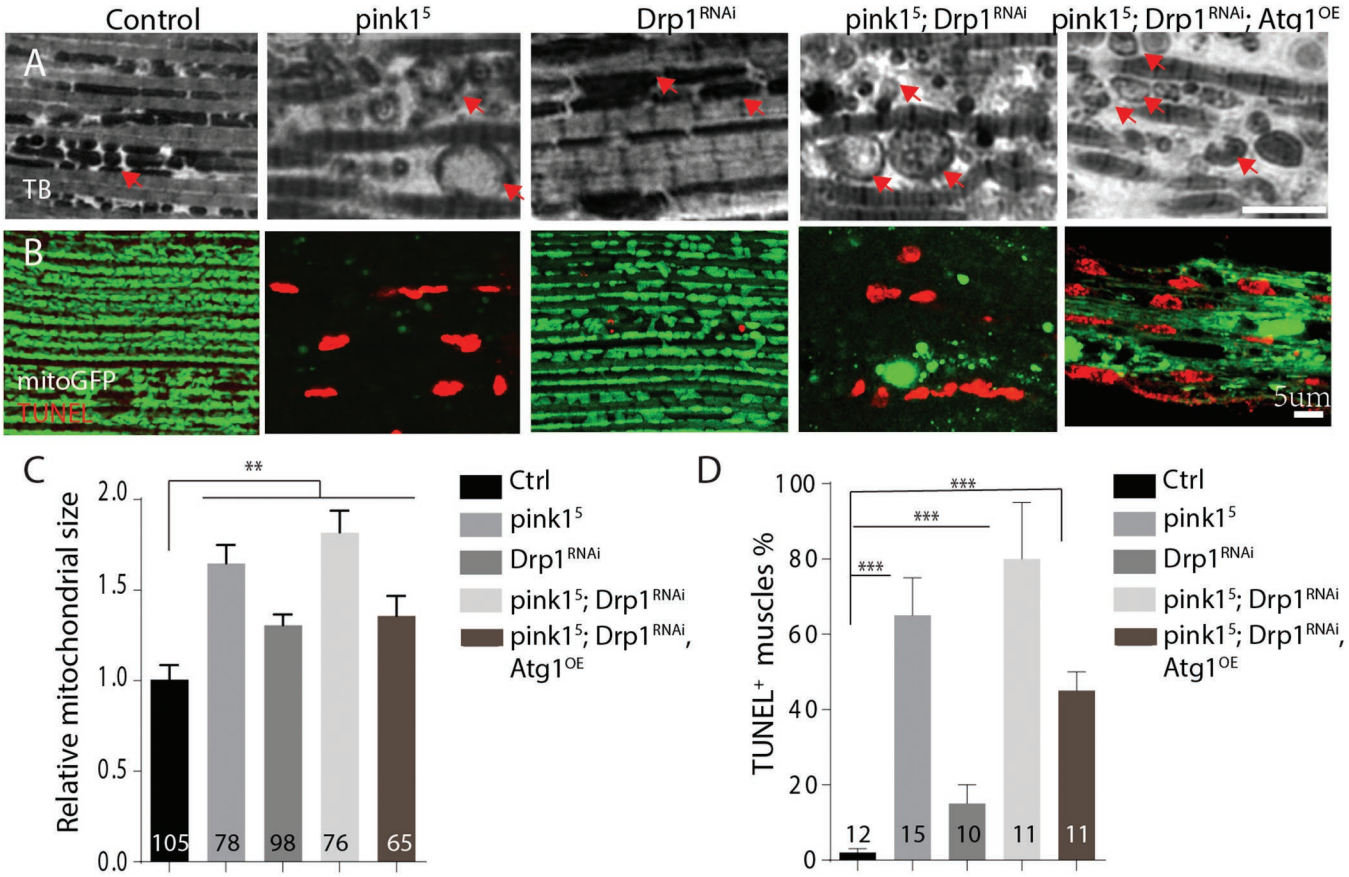

FIGURE 3: Atg1 overexpression rescues *pink1*^{5} pathogenesis by promoting mitochondrial fission. (A) Toluidine blue staining of thick muscle sections. Arrows point to typical mitochondria, which are swollen, with faint staining. (B) TUNEL staining (red) in indirect flight muscles and mitochondria visualized by mitoGFP. (C) Mitochondrial size of indicated genotypes was normalized and quantified mitochondria (number indicated in the chart) from at least 10 animals were analyzed. (D) Percentages of TUNEL-positive muscles were quantified. Number of animals used for each genotype is shown in the chart. For C, one-way ANOVA was performed for quantitative analysis, and for D, *t* tests were performed. SEM and *p* values are shown: ***$p < 0.001$, **$p < 0.01$, *$p < 0.05$.

Rab7 or components of the Vps-C complex resulted in accumulated aberrant large LysoTracker-positive structures in muscles (Supplemental Figure S6B; knockdown efficiency of RNA interference [RNAi] lines used in this study is shown in Supplemental Figure S7) and blockage of autophagy in *pink1*^{5} muscles (Figure 2, E–G, and Supplemental Figures S3–S5). Although knockdown of Rab7 or components of the Vps-C complex did not change mitochondrial morphology (Supplemental Figure S6C), they abrogated the rescue effect of Atg1^{OE}, as mito::GFP aggregates reappeared in *pink1*^{5} muscles (Figure 2G and Supplemental Figure S5). Inhibiting lysosomal acidification by *VhaAC39a* RNAi was also able to block the rescue effect of Atg1^{OE} (Figure 2G and Supplemental Figure S5). These results indicated that the autolysosomal pathway is required for Atg1^{OE}-mediated mitochondrial clearance in *pink1*^{5} muscles.

Atg1 overexpression rescues *pink1*^{5} pathogenesis by promoting mitochondrial fission

As indicated above, mitochondria are significantly smaller in Atg1^{OE} muscles, suggesting that Atg1 can regulate mitochondrial dynamics. Because mitochondrial fission is essential for maintaining mitochondria integrity and cell survival in *pink1*^{5} muscles (Deng *et al.*, 2008), we propose that mitochondrial dynamics is also required for the rescuing effect of Atg1^{OE}. Mitochondrial fission was inhibited by knocking down *Drp1* (Supplemental Figure S8). Consistent with previous results (Deng *et al.*, 2008), we did not observe mito::GFP clumps or TUNEL-positive nuclei in *Drp1* RNAi muscles, although mitochondria were slightly fused (Figure 3, A–D, and Supplemental Figure S8). However, knocking down *Drp1* in a *pink1*^{5} background exacerbated the mitochondrial morphological defects and the percentage of TUNEL-positive cell death (Figure 3D). Surprisingly, Atg1^{OE} no longer rescues *pink1*^{5} in the absence of *Drp1*, as mito-GFP clumps and TUNEL-positive nuclei reappeared (Figure 3, A–D). Also, the "fragmented" mitochondria in Atg1^{OE} were significantly restored by *Drp1* RNAi (Figure 4A and Supplemental Figure S9). On the other hand, knockdown of *Atg1* in muscles resulted in the accumulation of more mitochondria with irregular shapes, increased volume and size (Figure 4A and Supplemental Figure S9). Intriguingly, these irregularly elongated mitochondria in *Atg1* RNAi muscles were fully suppressed by *Drp1* overexpression (Figure 4A and Supplemental Figure S9). These results further indicated that Atg1 regulates mitochondrial dynamics.

We next tested whether Atg1 can regulate core components of the mitochondrial machinery. A mild increase in *drp1* transcripts was found in Atg1^{OE} muscles by RT-qPCR (Figure 4B). However, the Drp1 protein level increased two- to threefold in Atg1^{OE} muscles, as observed by anti-HA staining of Drp1-HA (HA-tagged Drp1 under an endogenous promoter; Figure 4, C and D). Significant increases of Drp1-HA foci were also found in Atg1^{OE} muscles (Figure 4E).

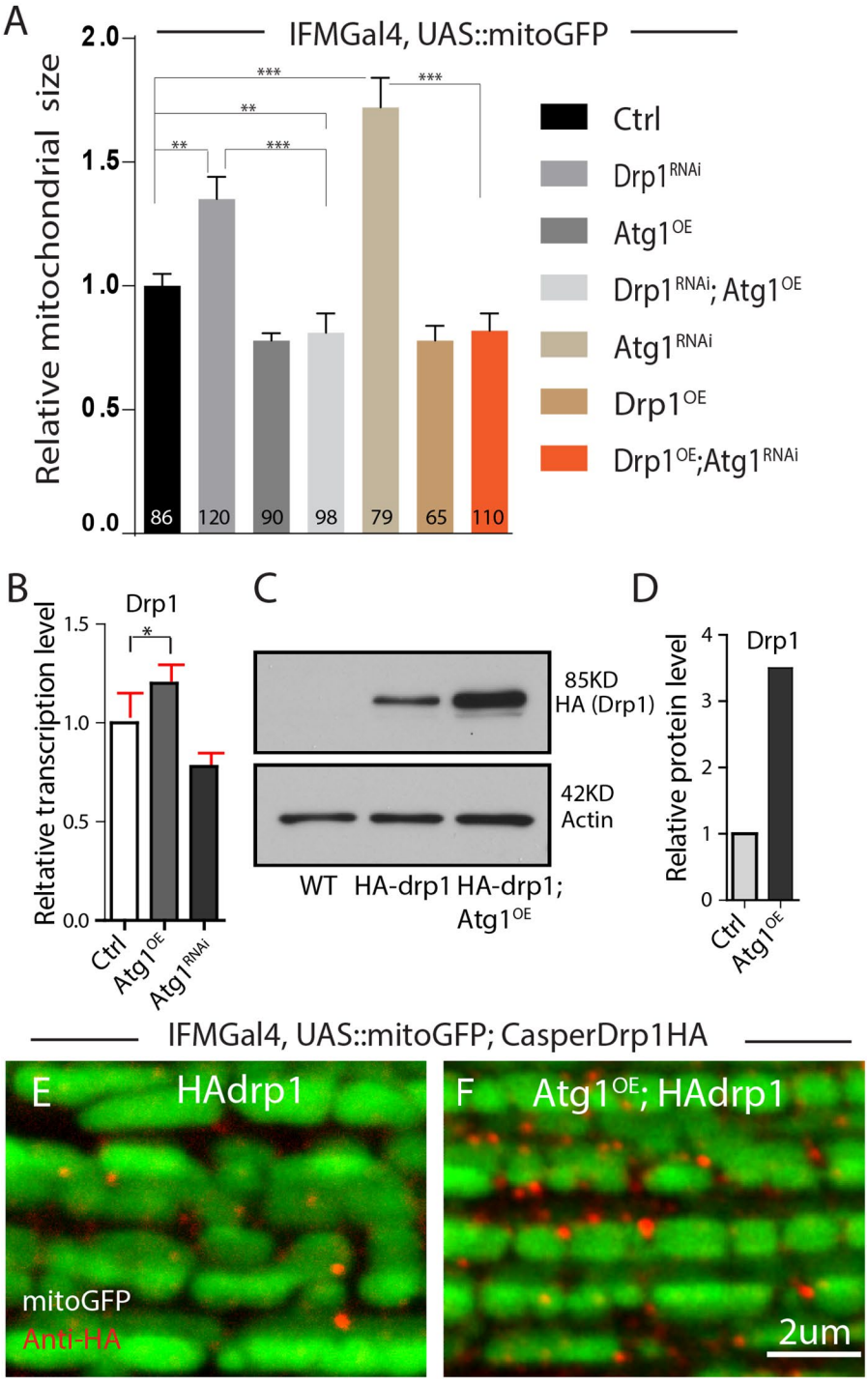

FIGURE 4: Atg1 regulates mitochondrial dynamics. (A) Quantifications of relative mitochondrial size. Mitochondrial size was normalized with controls. Mitochondria from at least 10 animals were analyzed (number indicated in the chart). (B) Relative transcription of *drp* was measured by RT-qPCR and normalized by actin-5C. Data represent triplicates of RNA samples from 10 thoraces for each genotype. (C) Western blot analysis of lysates from thorax by anti-HA antibody. No anti-HA signal was detected in flies without HA-Drp1 transgene. (D) Relative expression level of Drp1 was normalized by beta-actin based on Western blot results in F. (E). HA-tagged Drp1 protein (Drp1-HA) detected by anti-HA staining (red) in muscles. mito::GFP (green) marks mitochondria.

Taken together, these results indicate that Atg1 promotes mitochondrial fission at least partially through Drp1 and that *drp1* is required for the Atg1^{OE} rescue effect on *pink1*^{5} muscle degeneration.

Drp1 overexpression or *mfn* knockdown rescues *pink1*^{5} mitochondrial abnormality and muscle degeneration when autophagy and proteasome are impaired

We sought to test whether enhancing fission can rescue *pink1*^{5} pathogenesis when the degradation systems (proteasome/autophagy) are impaired. Lipidation of Atg8 (a homologue of LC3) is commonly used as a marker for autophagosomes (Kabeya *et al.*, 2000; Klionsky *et al.*, 2008). In young wild-type muscles (3–5 d old), Atg8::mCherry positive dots are smaller than mitochondria (<0.1 μm in diameter vs. 0.2–2 μm for mitochondria), and they rarely colocalized with mito::GFP (0/200 dots in muscles from 10 different flies; Supplemental Figures S3 and S10A). Knocking down *Atg1* in muscles suppressed Atg8::mCherry positive punctae in wild-type muscles (Supplemental Figure S10, A and B). Interestingly, although no signs of degeneration occurred in young *Atg1* RNAi muscles, *Atg1* RNAi accelerated the appearance of TUNEL positive muscles in *pink1*^{5} mutants (Figure 5, A and B), suggesting that autophagy is beneficial for cell survival. Strikingly, *pink1*^{5}-associated defects, such as mitochondrial abnormalities and TUNEL-positive cell death, were fully suppressed by overexpressing *drp1* in an *Atg1* RNAi background (Figure 5, A and B).

Age-dependent muscle degeneration in *pink1*^{5} was evaluated by TUNEL staining of hemithoraces. A significant increase of TUNEL-positive muscles was observed with age in *pink1*^{5} mutants (55% positive in 4-d-old vs. 80% in 20-d-old animals; Figure 5C). However, Drp1^{OE} sustains the rescue effect in 20-d-old *pink1*^{5} mutant muscles when Atg1 is simultaneously inhibited (Figure 5C).

In *Atg7*$^{d14/d77}$ transheterozygous mutant muscles, the mitochondria were largely normal and there was no obvious cell death (Figure 5A). Muscle degeneration in *pink1*^{5} worsened in an *Atg7*$^{d14/d77}$ background, as indicated by increasing TUNEL-positive muscles (Figure 5B). Interestingly, Drp1^{OE} also rescued *pink1*^{5} muscles in the absence of *Atg7* (Figure 5, A and B). Knocking down genes for downstream autophagy processes, such as Rab7 and Vha39AC, also failed to block the rescue effect of Drp1^{OE} on *pink1*^{5} muscle pathogenesis (unpublished data).

Inhibiting the proteasome activity by overexpressing DTS-7 (dominant temperature-sensitive mutation of the proteasome β2 subunit; Schweisguth, 1999; Belote and Fortier, 2002) and exposing the animals to the restrictive temperature (29°C) produced large ubiquitin-positive inclusion in muscles (Supplemental Figure S10, C and D). This indicated that DTS-7 can efficiently suppress proteasome activity. We found that DTS-7^{OE} deteriorated *pink1*^{5} muscle defects; however, it still failed to block the rescue effect of Drp1^{OE} (Figure 5, A and B).

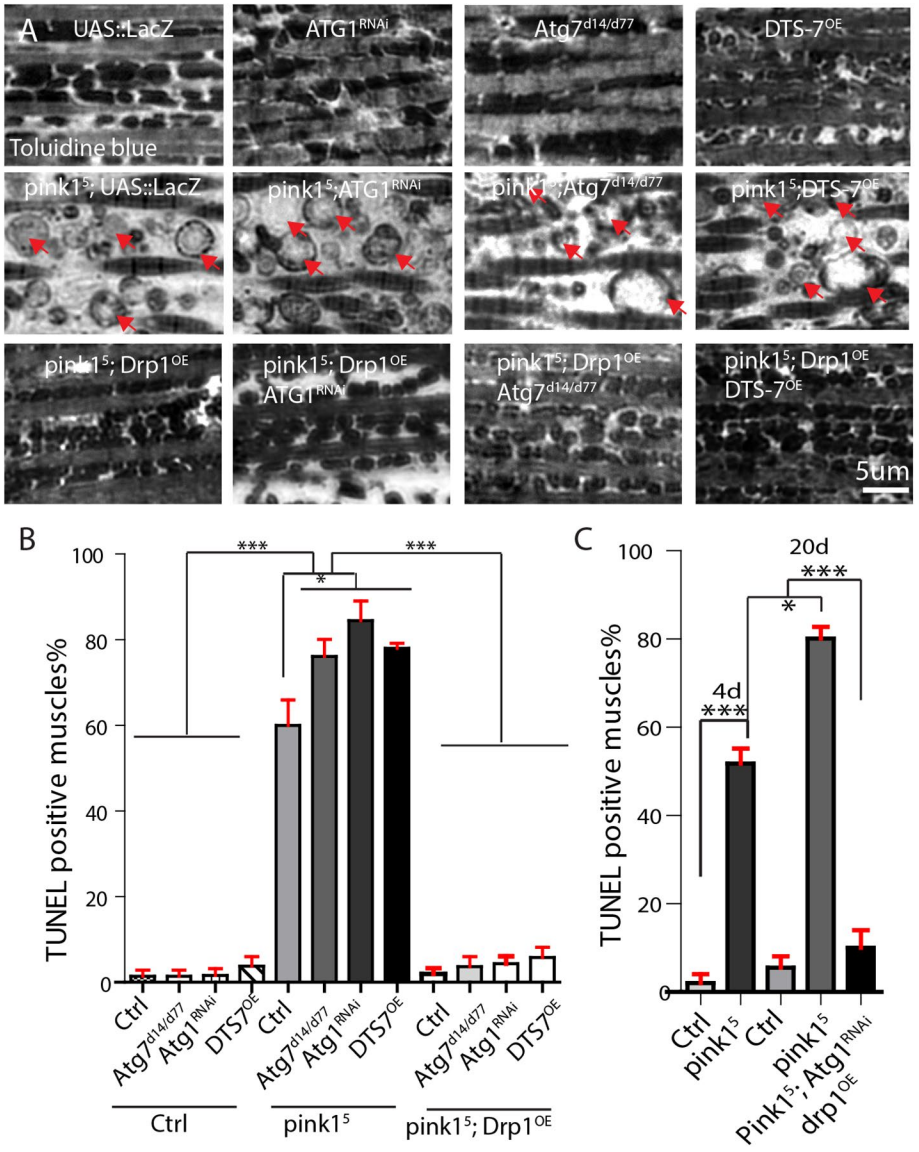

FIGURE 5: Overexpressing Drp1 rescues *pink1*^{5} muscle pathogenesis when autophagy or proteasome is impaired. (A) Genetic regulation of mitochondrial integrity in *pink1*^{5} mutant muscles. Mitochondria stained with toluidine blue (black dots). Arrows point to typical swollen, faintly stained mitochondria. (B) Quantification of TUNEL-positive muscles in the thoraces. Muscles from at least 10 hemithoraces of each genotype are dissected and stained by TUNEL assay. (C) Age-dependent increasing of TUNEL-positive muscles in *pink1*^{5} mutants rescued by Drp1 overexpression when autophagy was inhibited. Age of flies was included in the chart. Indirect flight muscles are multinucleated and the nuclei in *pink1*^{5} muscle are synchronized, that is, either all negative or all positive in terms of TUNEL staining. Student's *t* test for statistics. $*p < 0.05$ and $***p < 0.001$.

Mfn is a direct substrate of *pink1/parkin* in both *Drosophila* and mammalian cell lines (Poole *et al.*, 2010; Ziviani *et al.*, 2010; Chen and Dorn, 2013). Inhibiting fusion by knocking down *mfn* also rescues *pink1*^{5} pathogenesis under *Atg1*^{RNAi} or DTS-7^{OE} conditions (Supplemental Figure S11, A–D).

Drp1 overexpression rescues mitochondrial abnormalities and dopaminergic neuron loss in *pink1* RNAi brain when autophagy and the proteasome are defective

Progressive loss of dopaminergic (DA) neurons is one of the hallmarks of PD. *Pink1* and *parkin* mutants also experienced severe mitochondrial defects and dopaminergic neuron loss (Park *et al.*, 2006; Yang *et al.*, 2006, 2008; Poole *et al.*, 2008; Yun *et al.*, 2008, 2014). Mitochondria in DA neurons are normally elongated, but form clumps in a *pink1*^{RNAi} background, as indicated by mito::GFP driven by a DA neuron-specific driver, tyrosine hydroxylase (TH) GAL4 (Figure 6, A and B). *pink1*^{RNAi} flies encountered slight but significant loss of DA neurons, especially in the protocerebral posterior lateral 1 (PPL1) cluster (Park *et al.*, 2006; Poole *et al.*, 2008; Yang *et al.*, 2006; Figure 6C).

We sought to test the physiological relationship of autophagy and mitochondrial dynamics to DA neuron viability in *pink1*^{RNAi} flies. First, autophagic activity was examined in DA neurons. A few Atg8::mCherry-positive autophagosomes were observed in these neurons. Similarly to those found in muscles, these punctae barely colocalized with mito::GFP. Also, these Atg8::mCherry positive dots were substantially blocked by *Atg1*^{RNAi} in DA neurons, indicating that *Atg1*^{RNAi} suppresses autophagy efficiently in DA neurons. DA neurons with Drp1^{OE} have comparable Atg8-positive vesicles. On the other hand, DA neurons with *pink1*^{RNAi} had significantly larger, fused Atg8-positive vesicles, and these vesicles partially associated with mito::GFP (Figure 6A).

Atg1^{RNAi} in DA neurons had no obvious defects in mitochondrial morphology, and the cell numbers in the PPL1 cluster were comparable to those in the controls. However, the mito::GFP clumps and cell loss in PPL1 cluster in *pink1*^{RNAi} flies were further exacerbated by *Atg1*^{RNAi} in DA neurons (Figure 6, B and C). Drp1 overexpression fully rescues mito::GFP clumps and degeneration in DA neurons of *pink1*^{RNAi} flies. Moreover, the rescuing effects were sustained in the *Atg1*^{RNAi} background (Figure 6, B and C). Similarly, inhibiting fusion by knocking down mfn could also significantly rescue mito::GFP clumps in *pink1*^{RNAi} flies, even when *atg1*^{RNAi} was silenced simultaneously (Figure 6, B and C).

These results suggested that, in contrast to the degradative processes, enhancing fission or inhibiting fusion is essential for cell survival in *pink1/parkin* mutants.

DISCUSSION

Recent studies of mammalian cell lines implicated that *pink1/parkin*-mediated mitophagy is crucial for mitochondrial quality control. In brief, Pink1 is stabilized on heavily uncoupled mitochondria and recruits Parkin. Ubiquitination of mitochondrial outer membrane proteins facilitates subsequent turnover of the mitochondria by proteolysis and autophagy. However, the physiological contribution of mitophagy to *pink1/parkin* null-mediated pathogenesis is elusive.

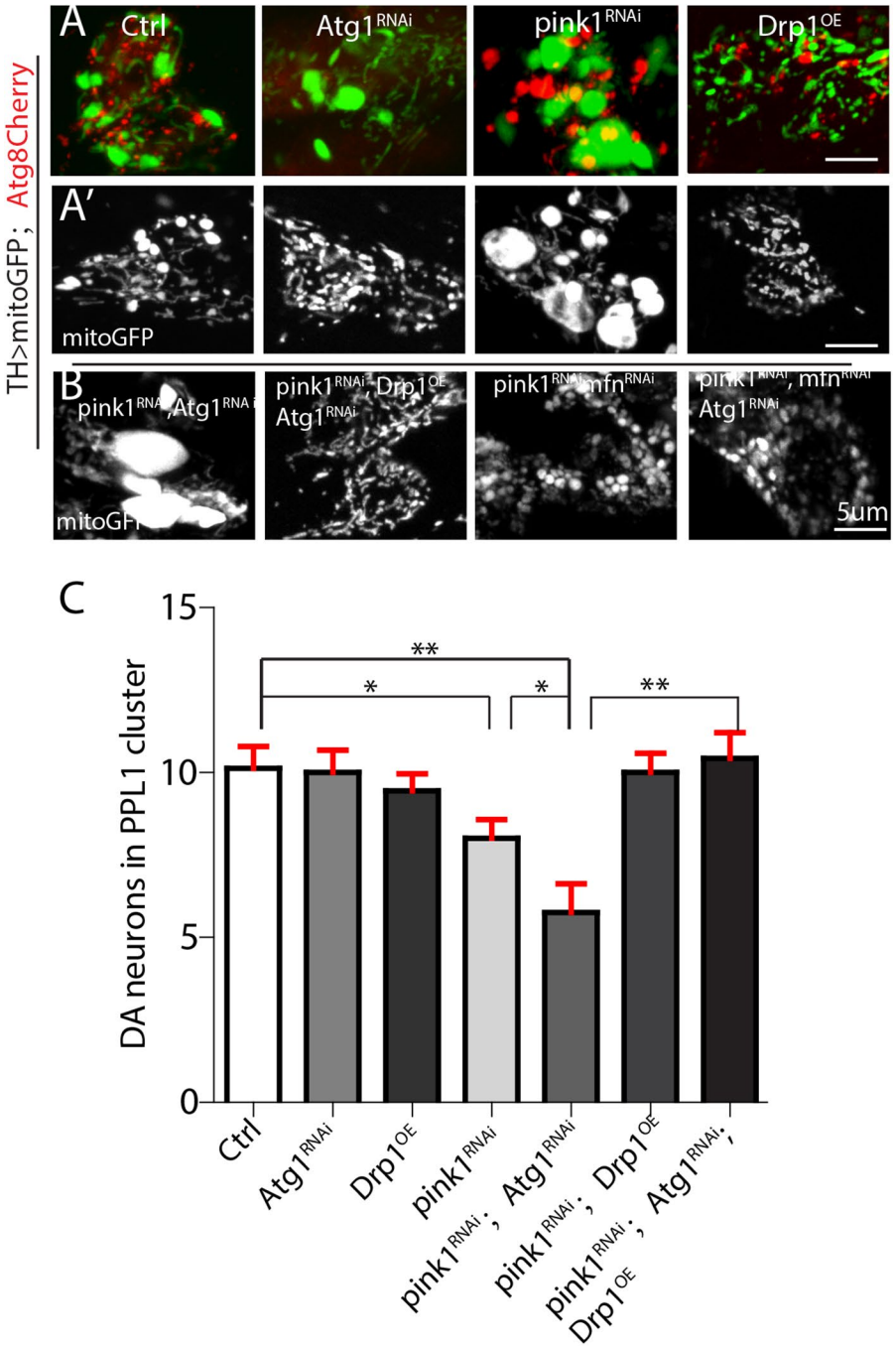

FIGURE 6: Overexpressing Drp1 rescues mitochondrial defects and dopaminergic (DA) neuron loss in *pink1*^{5} mutants when autophagy or proteasome is impaired.
(A) Autophagosomes in DA neurons were visualized by UAS::Atg8::mCherry under the driver TH-Gal4, where mitochondria are labeled by mito::GFP in green. A′ is the mitoGFP channel in gray. (B) Genetic analysis of mitochondrial morphology in DA neurons is represented by TH-Gal4 > mitoGFP in gray. (C) Quantification of DA neuron cell number in PPL1 clusters. DA neurons were labeled by THGal4 > CD8::GFP. PPL1 regions of 10 brains for each genotype were counted. Average standard error is shown and statistics were performed by Student's *t* test. *$p < 0.05$, **$p < 0.01$.

Autophagy is a catabolic process that helps maintain energy balance by recycling cellular compartments. Our data indicated that enhancing autophagy was generally beneficial for flies lacking *pink1/parkin*, which is consistent with a recent finding (Liu and Lu, 2010). However, we were not able to recapitulate the mitophagy process in *Drosophila*. First, under physiological conditions, there are only a few autophagosomes (marked by Atg8::mCherry) in these tissues, and these dots were never colocalized with mitochondria (labeled with mito::GFP). Second, mitochondrial uncoupling, either by feeding the flies with CCCP (carbonyl cyanide *m*-chlorophenyl hydrazine) or by genetically overexpressing hUCP2 (Fridell *et al.*, 2005), failed to increase the colocalization of Atg8::mCherry and mito::GFP (0/300 dots in muscles from 12 different flies; unpublished data). Finally, no obvious Pink1 stabilization or Parkin recruitment was observed after mitochondrial uncoupling (Supplemental Figure S12, A–F). Consistent with our results, a recent paper also failed to detect a role of *pink1/parkin* in mitophagy in *Drosophila* (Lee *et al.*, 2018).

Why was mitophagy not observed in *Drosophila* muscles? It might be simply because mitophagy happens rarely, or occurs extremely fast or slowly, and these events failed to be detected in the current experimental settings. Indeed, Parkin recruitment to uncoupled mitochondria is substantially different in fibroblasts from that in neurons in terms of kinetics and extent (4 h after CCCP treatment, 70% recruitment in neurons; 2 h, 100% recruitment in fibroblasts; Seibler *et al.*, 2011; Van Laar *et al.*, 2011). Alternatively, mitophagy might only become prominent after extreme mitochondrial insults. Here, we found mitochondrial depolarization only after prolonged high-dose CCCP feeding (Supplemental Figure S12, G and H). It is quite possible that the buffering capacity of mitochondria in different tissues may vary; delivery method and timing may also alter the feeding effect of CCCP in vivo. In fact, *pink1/parkin*-mediated mitophagy relies heavily on severe mitochondrial uncoupling, such as FCCP/CCCP. How it compares with physiological mitochondrial dysfunction is unknown (de Vries *et al.*, 2012; Grenier *et al.*, 2013). In fact, in a mouse model deficient for the mitochondrial transcription factor A, no parkin recruitment to mitochondria was observed in the brain (Sterky *et al.*, 2011). It was proposed that both mitochondrial dynamics and mitochondrial autophagy contribute to mitochondrial quality control (Twig and Shirihai, 2011; McCoy and Cookson, 2012; Ashrafi and Schwarz, 2013): mitochondrial fission facilitates the segregation of severely damaged mitochondria, which are then selectively eaten up by autophagy machinery. Mitochondrial fission facilitates mitophagy, since blocking fission by a dominant negative form of Drp1 impairs the mitophagy process (Dagda *et al.*, 2009; Frank *et al.*, 2012; Rana *et al.*, 2017). *Pink1* and *parkin* are required in mitochondrial quality control, since they regulate both processes. If these two processes are physiologically linked, we

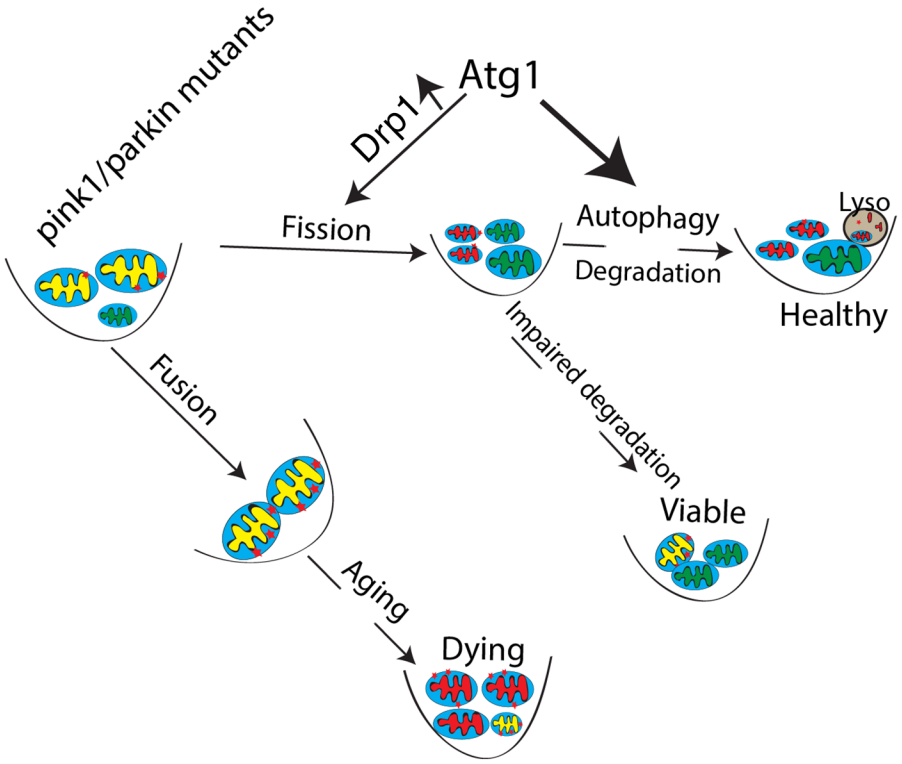

FIGURE 7: Dual beneficial roles of Atg1 in *pink1/parkin* pathogenesis. In *pink1/parkin* mutants, mitochondria are dysfunctional (colored in yellow). Mitochondrial fission helps to segregate "severely" damaged mitochondria (red ones) and is crucial for mitochondrial quality control and cell survival in *pink1/parkin* mutants. Overexpressing Atg1 is beneficial at least in two ways. On one hand, it promotes fission through Drp1, which would help to pinch off the "damaged" portion of "bad" mitochondria (red); on the other hand, it accelerates autophagic degradation of severely damaged mitochondria. When degradation machinery is impaired, "healthier" mitochondria (green) generated by elevated fission are sufficient for cell survival.

would assume that both processes would be essential for pink1/parkin null related pathogenesis.

However, we found here that increasing fission or inhibiting fusion can still rescue *pink1/parkin* muscle degeneration when the autophagy or proteasome activity was hampered. Hence, we propose that, although clearance of severely damaged mitochondria by autophagy is beneficial, a subset of healthy mitochondria segregated by mitochondrial fission was sufficient to maintain cellular health and tissue survival in *pink1/parkin* mutants (Figure 7).

Atg1 is a highly conserved Ser/Thr kinase that plays an essential role in autophagy. Substrates of this kinase identified so far, such as Atg13 and Atg9, are components of the autophagy pathway (Chang and Neufeld, 2009; Papinski *et al.*, 2014). Here we found that Atg1 can promote mitochondrial fission at least partially through Drp1. How does Atg1 regulate Drp1 protein levels? Posttranscriptional modifications, such as phosphorylation, can modulate Drp1 activity and hence mitochondrial morphology. Thus, Atg1 might directly or indirectly modify Drp1 posttranscriptionally.

Atg1 activity is tightly regulated by the nutrition-sensing mTOR pathway (Chang and Neufeld, 2009; Mizushima, 2010). Mitochondrial dynamics and mitochondrial metabolic activity are also regulated by nutrition status (Liesa and Shirihai, 2013). Our results suggested that Atg1 might coordinate mitochondrial dynamics and autophagy activity to cope with the nutritional status of cells (Figure 7). The dual role of Atg1 in mitochondrial dynamics and autophagy makes it a hotspot for mitochondrial quality control.

MATERIALS AND METHODS

Drosophila genetics and strains

UAS-Atg1^{6A}, UAS-Atg1^{KQ}, Atg7^{d14}, Atg7^{d77}, and UAS-Atg8-mCherry flies were obtained from Thomas Neufeld, CaSpeR-HA-drp1 from Hugo J Bellen, and UAS-hUCP2 from Stephen L. Helfand. Atg1RNAi (BL44034), UAS::Rab7 RNAi (BL 27051), UASp::Rab7::GFP(BL23641), UAS-mitoGFP, Mef2-GAL4, and TH-GAL4 flies were obtained from the Bloomington Drosophila Stock Center. IFM-GAL4, *Pink1*^{5}, *parkin*^{25}, *dpk*^{21}, UAS-*Drp1*, UAS-*Drp1* RNAi, and UAS-*mfn* RNAi flies have been described previously (Deng *et al.*, 2008; Yun *et al.*, 2014). *Drosophila* strains were raised on standard medium at 25°C with 12 h day/night cycle unless otherwise specified.

RNA isolation, cDNA synthesis, and RT-qPCR

RNA was isolated from thorax by Trizol. cDNA synthesis was performed using a combination of Oligo-dT and random hexamer priming by the Clontech RNA to cDNA EcoDry Premix Kit. Quantitative RT-PCR was performed using the BioRad iTaq Fast Sybr Green enzyme mix, 10-µl reactions in triplicate, on a Roche Light Cycler 480. Standard curves were generated for targets and normalized with the control gene Actin-5C. *t* test and SEM. were performed for statistical analysis. ***: p value < 0.001. Primers used in this study:

Actin5C (F): 5′-CTCGCCACTTGCGTTTACAGT-3′, Actin5C (R): 5′-TCCATATCGTCCCAGTTGGTC-3′

Drp1 (F): 5′-GGCCCTAATTCCGGTCATAAA-3′, Drp1(R):5′-CTCTGACTGCCTAGAACAACAA-3′

Car (CG12230) (F) 5′-GATGCACGTTCGCTGAAATAG-3′, (R) 5′-GTCCAGGAAGGAGTGTTTGT-3′

Atg1 (CG10967) (F) 5′-AGCCTGGTCATGGAGTATTG-3′, (R) 5′-GTTGCACGAGGAAGAGTCTAA-3′

Rab7 (CG5915) (F) 5′-CAAACGCTTCTCCAACCAATAC-3′ (R) 5′-AGATCTGCATTGTGACCACTC-3′

VhaAC39-1 (CG2934) (F) 5′-CAGACCCAAGCCTAGATTTCTC-3′ (R) 5′-ACTATGGGTCTCCCGAATACA

Immunofluorescence and confocal microscopy

For muscles, thoraces were dissected and fixed in 4% paraformaldehyde in phosphate-buffered saline (PBS). After thoraces were washed three times in PBS, muscle fibers were isolated and stained with rhodamine phalloidin (Invitrogen; 1:1000) in PBS + 1% Triton X-100. For antibody staining, muscle fibers were permeabilized and blocked in PBS + 0.1% Triton X-100 and incubated in primary and secondary antibodies diluted in PBS + 1% bovine serum albumin (BSA). The following primary antibodies were used: chicken anti-HA (Millipore, Billerica, CA), mouse anti- ATP Synthase (Mitosciences, Eugene, OR), and mouse anti-myc (Sigma, MO). For DA neurons, brains of 3-d-old male flies were dissected and fixed in 4%

paraformaldehyde in PBS. All images were taken on a Zeiss LSM5 confocal microscope.

TUNEL assay and quantification

Thoraces from adult male flies were dissected and fixed in 4% paraformaldehyde in PBS. Muscle fibers were isolated and subsequently permeabilized and blocked in T-TBS-3% BSA (T-TBS: 0.1% Triton X-100, 50 mM Tris-Cl [pH 7.4], and 188 mM NaCl). After blocking, TUNEL staining was carried out using an In-Situ Cell Death Detection Kit from Roche. Percentages of TUNEL-positive muscles are quantified based on muscle fibers from at least 10 flies in each genotype. For TUNEL-positive muscles quantification, hemithoraces were dissected and prepared as previously reported (Schonbauer *et al.*, 2011). After fixation and permeabilization, TUNEL assays were performed. At least 50–60 muscles from 10 thoraces were examined for each genotype.

Mitochondrial size measurement

Mitochondrial in muscles of indicated genotypes were labeled with mitochondrial-targeted GFP (mitoGFP) and imaged by confocal microscopy under the same setting.

Individual mitochondria were then circled out and the volume of ROI was measured with ImageJ. At least 100 mitochondria from 10 animals were analyzed. *t* tests were performed for statistical analysis.

Analysis of dopaminergic neurons

Fly brains were dissected from 25-d-old male flies. Dopaminergic neurons were labeled with anti-tyrosine hydroxylase staining. Brains were imaged by confocal microscopy and PPL1 cluster neurons were counted per brain hemisphere. Data were analyzed by Prism 5 software from at least 10 brains for each genotype.

Embedding, sections, toluidine blue staining, and TEM

Thoraces from young male flies were dissected, fixed in paraformaldehyde/glutaraldehyde, postfixed in osmium tetraoxide, dehydrated in ethanol, and embedded in Epon. After polymerization of Epon, blocks were cut to generate 1.5 µm–thick sections using a glass knife, or 80 nm–thick sections using a diamond knife on a microtome (Leica, Germany). Toluidine blue was used to stain 1.5 µm–thick tissue sections. Thin sections (80 nm thick) were stained with uranyl acetate and lead citrate and then examined using a JEOL 100C transmission electron microscope (UCLA Brain Research Institute Electron Microscopy Facility). At least six thoraces were examined in each sample.

Drosophila lysate preparation and Western blotting

Thoraces from adult flies were homogenized in RIPA buffer containing protease inhibitors (Roche). Total protein concentration was measured using a Bradford assay kit (Bio-Rad, Hercules, CA), and the same amount of protein was loaded onto SDS–polyacrylamide gels. The following primary antibodies were used for Western blots: mouse anti-HA (Millipore) and rabbit anti-Actin (Sigma).

LysoTracker and TMRE staining

Muscles was freshly dissected in PBS and incubated in a dark chamber within which PBS contains 1/1000 diluted LysoTracker Red DND-99 (Life Technologies) or 1 µM TMRE (dissolved in 100% ethanol, from Molecular Probes) for 30 min. After brief rinsing and washing in PBS, muscles were mounted in PBS and immediately imaged under microscopy.

ACKNOWLEDGMENTS

This work was supported by a National Key Research and Development Project (2018YFA0107100), the Youth 1000 Talent Plan of China and Tongji University Basic Scientific Research-Interdisciplinary Fund to H.D., the National Institutes of Health (R01), the McKnight Neuroscience Foundation, the Kenneth Glenn Family Foundation, the Natalie R and Eugene S Jones Fund in Aging and Neurodegenerative Disease Research to M.G. and an Ellison Medical Foundation Senior Scholar Award and funds from the UCLA Laurie and Steven Gordon Commitment to Cure Parkinson's Disease to M.G. We thank Hugo Bellen, Thomas Neufeld, and Stephen Helfand for flies, Michael Lizzio for technical assistance, and Frank Laski and Volker Hartenstein for the use of their equipment.

REFERENCES

Ashrafi G, Schwarz TL (2013). The pathways of mitophagy for quality control and clearance of mitochondria. Cell Death Differ 20, 31–42.

Belote JM, Fortier E (2002). Targeted expression of dominant negative proteasome mutants in *Drosophila melanogaster*. Genesis 34, 80–82.

Brand AH, Perrimon N (1993). Targeted gene expression as a means of altering cell fates and generating dominant phenotypes. Development 118, 401–415.

Chan NC, Salazar AM, Pham AH, Sweredoski MJ, Kolawa NJ, Graham RL, Hess S, Chan DC (2011). Broad activation of the ubiquitin-proteasome system by Parkin is critical for mitophagy. Hum Mol Genet 20, 1726–1737.

Chang YY, Neufeld TP (2009). An Atg1/Atg13 complex with multiple roles in TOR-mediated autophagy regulation. Mol Biol Cell 20, 2004–2014.

Chen H, Chan DC (2009). Mitochondrial dynamics—fusion, fission, movement, and mitophagy—in neurodegenerative diseases. Hum Mol Genet 18, R169–R176.

Chen Y, Dorn GW 2nd (2013). PINK1-phosphorylated mitofusin 2 is a Parkin receptor for culling damaged mitochondria. Science 340, 471–475.

Chen Y, Klionsky DJ (2011). The regulation of autophagy—unanswered questions. J Cell Sci 124, 161–170.

Clark IE, Dodson MW, Jiang C, Cao JH, Huh JR, Seol JH, Yoo SJ, Hay BA, Guo M (2006). *Drosophila* pink1 is required for mitochondrial function and interacts genetically with parkin. Nature 441, 1162–1166.

Dagda RK, Cherra SJ 3rd, Kulich SM, Tandon A, Park D, Chu CT (2009). Loss of PINK1 function promotes mitophagy through effects on oxidative stress and mitochondrial fission. J Biol Chem 284, 13843–13855.

de Vries RL, Gilkerson RW, Przedborski S, Schon EA (2012). Mitophagy in cells with mtDNA mutations: being sick is not enough. Autophagy 8, 699–700.

Deng H, Dodson MW, Huang H, Guo M (2008). The Parkinson's disease genes pink1 and parkin promote mitochondrial fission and/or inhibit fusion in *Drosophila*. Proc Natl Acad Sci USA 105, 14503–14508.

Exner N, Treske B, Paquet D, Holmstrom K, Schiesling C, Gispert S, Carballo-Carbajal I, Berg D, Hoepken HH, Gasser T, *et al.* (2007). Loss-of-function of human PINK1 results in mitochondrial pathology and can be rescued by parkin. J Neurosci 27, 12413–12418.

Flinn L, Mortiboys H, Volkmann K, Koster RW, Ingham PW, Bandmann O (2009). Complex I deficiency and dopaminergic neuronal cell loss in parkin-deficient zebrafish (*Danio rerio*). Brain 132, 1613–1623.

Frank M, Duvezin-Caubet S, Koob S, Occhipinti A, Jagasia R, Petcherski A, Ruonala MO, Priault M, Salin B, Reichert AS (2012). Mitophagy is triggered by mild oxidative stress in a mitochondrial fission dependent manner. Biochim Biophys Acta 1823, 2297–2310.

Fridell YW, Sanchez-Blanco A, Silvia BA, Helfand SL (2005). Targeted expression of the human uncoupling protein 2 (hUCP2) to adult neurons extends life span in the fly. Cell Metab 1, 145–152.

Gautier CA, Kitada T, Shen J (2008). Loss of PINK1 causes mitochondrial functional defects and increased sensitivity to oxidative stress. Proc Natl Acad Sci USA 105, 11364–11369.

Grenier K, McLelland GL, Fon EA (2013). Parkin- and PINK1-dependent mitophagy in neurons: will the real pathway please stand up? Front Neurol 4, 100.

He C, Klionsky DJ (2009). Regulation mechanisms and signaling pathways of autophagy. Annu Rev Genet 43, 67–93.

Hyttinen JM, Niittykoski M, Salminen A, Kaarniranta K (2013). Maturation of autophagosomes and endosomes: a key role for Rab7. Biochim Biophys Acta 1833, 503–510.

Jager S, Bucci C, Tanida I, Ueno T, Kominami E, Saftig P, Eskelinen EL (2004). Role for Rab7 in maturation of late autophagic vacuoles. J Cell Sci 117, 4837–4848.
Juhasz G, Erdi B, Sass M, Neufeld TP (2007). Atg7-dependent autophagy promotes neuronal health, stress tolerance, and longevity but is dispensable for metamorphosis in *Drosophila*. Genes Dev 21, 3061–3066.
Kabeya Y, Mizushima N, Ueno T, Yamamoto A, Kirisako T, Noda T, Kominami E, Ohsumi Y, Yoshimori T (2000). LC3, a mammalian homologue of yeast Apg8p, is localized in autophagosome membranes after processing. EMBO J 19, 5720–5728.
Kawajiri S, Saiki S, Sato S, Sato F, Hatano T, Eguchi H, Hattori N (2010). PINK1 is recruited to mitochondria with parkin and associates with LC3 in mitophagy. FEBS Lett 584, 1073–1079.
Klionsky DJ, Abeliovich H, Agostinis P, Agrawal DK, Aliev G, Askew DS, Baba M, Baehrecke EH, Bahr BA, Ballabio A, *et al*. (2008). Guidelines for the use and interpretation of assays for monitoring autophagy in higher eukaryotes. Autophagy 4, 151–175.
Lee JJ, Sanchez-Martinez A, Zarate AM, Beninca C, Mayor U, Clague MJ, Whitworth AJ (2018). Basal mitophagy is widespread in *Drosophila* but minimally affected by loss of Pink1 or parkin. J Cell Biol 217, 1613–1622.
Liesa M, Shirihai OS (2013). Mitochondrial dynamics in the regulation of nutrient utilization and energy expenditure. Cell Metab 17, 491–506.
Liu S, Lu B (2010). Reduction of protein translation and activation of autophagy protect against PINK1 pathogenesis in *Drosophila melanogaster*. PLoS Genet 6, e1001237.
Lutz AK, Exner N, Fett ME, Schlehe JS, Kloos K, Lammermann K, Brunner B, Kurz-Drexler A, Vogel F, Reichert AS, *et al*. (2009). Loss of parkin or PINK1 function increases Drp1-dependent mitochondrial fragmentation. J Biol Chem 284, 22938–22951.
Matsuda N, Sato S, Shiba K, Okatsu K, Saisho K, Gautier CA, Sou YS, Saiki S, Kawajiri S, Sato F, *et al*. (2010). PINK1 stabilized by mitochondrial depolarization recruits Parkin to damaged mitochondria and activates latent Parkin for mitophagy. J Cell Biol 189, 211–221.
Mauvezin C, Nagy P, Juhasz G, Neufeld TP (2015). Autophagosome-lysosome fusion is independent of V-ATPase-mediated acidification. Nat Commun 6, 7007.
McCoy MK, Cookson MR (2012). Mitochondrial quality control and dynamics in Parkinson's disease. Antioxid Redox Signal 16, 869–882.
Mizushima N (2010). The role of the Atg1/ULK1 complex in autophagy regulation. Curr Opin Cell Biol 22, 132–139.
Narendra DP, Jin SM, Tanaka A, Suen DF, Gautier CA, Shen J, Cookson MR, Youle RJ (2010). PINK1 is selectively stabilized on impaired mitochondria to activate Parkin. PLoS Biol 8, e1000298.
Nelson N (2003). A journey from mammals to yeast with vacuolar H+-ATPase (V-ATPase). J Bioenerg Biomembr 35, 281–289.
Palacino JJ, Sagi D, Goldberg MS, Krauss S, Motz C, Wacker M, Klose J, Shen J (2004). Mitochondrial dysfunction and oxidative damage in parkin-deficient mice. J Biol Chem 279, 18614–18622.
Papinski D, Schuschnig M, Reiter W, Wilhelm L, Barnes CA, Maiolica A, Hansmann I, Pfaffenwimmer T, Kijanska M, Stoffel I, *et al*. (2014). Early steps in autophagy depend on direct phosphorylation of Atg9 by the Atg1 kinase. Mol Cell 53, 471–483.
Park J, Lee SB, Lee S, Kim Y, Song S, Kim S, Bae E, Kim J, Shong M, Kim JM, Chung J (2006). Mitochondrial dysfunction in *Drosophila* PINK1 mutants is complemented by parkin. Nature 441, 1157–1161.
Poole AC, Thomas RE, Andrews LA, McBride HM, Whitworth AJ, Pallanck LJ (2008). The PINK1/Parkin pathway regulates mitochondrial morphology. Proc Natl Acad Sci USA 105, 1638–1643.
Poole AC, Thomas RE, Yu S, Vincow ES, Pallanck L (2010). The mitochondrial fusion-promoting factor mitofusin is a substrate of the PINK1/parkin pathway. PLoS One 5, e10054.
Rana A, Oliveira MP, Khamoui AV, Aparicio R, Rera M, Rossiter HB, Walker DW (2017). Promoting Drp1-mediated mitochondrial fission in midlife prolongs healthy lifespan of *Drosophila melanogaster*. Nat Commun 8, 448.
Schapira AH (1993). Mitochondrial complex I deficiency in Parkinson's disease. Adv Neurol 60, 288–291.
Schapira AH (2008). Mitochondria in the aetiology and pathogenesis of Parkinson's disease. Lancet Neurol 7, 97–109.
Schonbauer C, Distler J, Jahrling N, Radolf M, Dodt HU, Frasch M, Schnorrer F (2011). Spalt mediates an evolutionarily conserved switch to fibrillar muscle fate in insects. Nature 479, 406–409.
Schweisguth F (1999). Dominant-negative mutation in the beta2 and beta6 proteasome subunit genes affect alternative cell fate decisions in the *Drosophila* sense organ lineage. Proc Natl Acad Sci USA 96, 11382–11386.
Scott RC, Juhasz G, Neufeld TP (2007). Direct induction of autophagy by Atg1 inhibits cell growth and induces apoptotic cell death. Curr Biol 17, 1–11.
Seibler P, Graziotto J, Jeong H, Simunovic F, Klein C, Krainc D (2011). Mitochondrial Parkin recruitment is impaired in neurons derived from mutant PINK1 induced pluripotent stem cells. J Neurosci 31, 5970–5976.
Sevrioukov EA, He JP, Moghrabi N, Sunio A, Kramer H (1999). A role for the deep orange and carnation eye color genes in lysosomal delivery in *Drosophila*. Mol Cell 4, 479–486.
Sriram V, Krishnan KS, Mayor S (2003). deep-orange and carnation define distinct stages in late endosomal biogenesis in *Drosophila melanogaster*. J Cell Biol 161, 593–607.
Sterky FH, Lee S, Wibom R, Olson L, Larsson NG (2011). Impaired mitochondrial transport and Parkin-independent degeneration of respiratory chain-deficient dopamine neurons in vivo. Proc Natl Acad Sci USA 108, 12937–12942.
Tatsuta T, Langer T (2008). Quality control of mitochondria: protection against neurodegeneration and ageing. EMBO J 27, 306–314.
Twig G, Elorza A, Molina AJ, Mohamed H, Wikstrom JD, Walzer G, Stiles L, Haigh SE, Katz S, Las G, *et al*. (2008). Fission and selective fusion govern mitochondrial segregation and elimination by autophagy. EMBO J 27, 433–446.
Twig G, Shirihai OS (2011). The interplay between mitochondrial dynamics and mitophagy. Antioxid Redox Signal 14, 1939–1951.
Van Laar VS, Arnold B, Cassady SJ, Chu CT, Burton EA, Berman SB (2011). Bioenergetics of neurons inhibit the translocation response of Parkin following rapid mitochondrial depolarization. Hum Mol Genet 20, 927–940.
Wang X, Winter D, Ashrafi G, Schlehe J, Wong YL, Selkoe D, Rice S, Steen J, LaVoie MJ, Schwarz TL (2011). PINK1 and Parkin target Miro for phosphorylation and degradation to arrest mitochondrial motility. Cell 147, 893–906.
Westermann B (2010). Mitochondrial fusion and fission in cell life and death. Nat Rev Mol Cell Biol 11, 872–884.
Whitworth AJ, Pallanck LJ (2017). PINK1/Parkin mitophagy and neurodegeneration-what do we really know in vivo? Curr Opin Genet Dev 44, 47–53.
Yan Y, Denef N, Schupbach T (2009). The vacuolar proton pump, V-ATPase, is required for notch signaling and endosomal trafficking in *Drosophila*. Dev Cell 17, 387–402.
Yang Y, Gehrke S, Imai Y, Huang Z, Ouyang Y, Wang JW, Yang L, Beal MF, Vogel H, Lu B (2006). Mitochondrial pathology and muscle and dopaminergic neuron degeneration caused by inactivation of *Drosophila* Pink1 is rescued by Parkin. Proc Natl Acad Sci USA 103, 10793–10798.
Yang Y, Ouyang Y, Yang L, Beal MF, McQuibban A, Vogel H, Lu B (2008). Pink1 regulates mitochondrial dynamics through interaction with the fission/fusion machinery. Proc Natl Acad Sci USA 105, 7070–7075.
Youle RJ, van der Bliek AM (2012). Mitochondrial fission, fusion, and stress. Science 337, 1062–1065.
Yu W, Sun Y, Guo S, Lu B (2011). The PINK1/Parkin pathway regulates mitochondrial dynamics and function in mammalian hippocampal and dopaminergic neurons. Hum Mol Genet 20, 3227–3240.
Yun J, Cao JH, Dodson MW, Clark IE, Kapahi P, Chowdhury RB, Guo M (2008). Loss-of-function analysis suggests that Omi/HtrA2 is not an essential component of the pink1/parkin pathway in vivo. J Neurosci 28, 14500–14510.
Yun J, Puri R, Yang H, Lizzio MA, Wu C, Sheng ZH, Guo M (2014). MUL1 acts in parallel to the PINK1/parkin pathway in regulating mitofusin and compensates for loss of PINK1/parkin. Elife 3, e01958.
Ziviani E, Tao RN, Whitworth AJ (2010). *Drosophila* parkin requires PINK1 for mitochondrial translocation and ubiquitinates mitofusin. Proc Natl Acad Sci USA 107, 5018–5023.